NANO LETTERS

Letter

pubs.acs.org/NanoLett

Oscillating Magnetoresistance in Graphene p−n Junctions at Intermediate Magnetic Fields

Hiske Overweg,*[,†] Hannah Eggimann,[†] Ming-Hao Liu,[‡,§] Anastasia Varlet,[†] Marius Eich,[†] Pauline Simonet,[†] Yongjin Lee,[†] Kenji Watanabe,[∥] Takashi Taniguchi,[∥] Klaus Richter,[‡] Vladimir I. Fal'ko,[⊥] Klaus Ensslin,[†] and Thomas Ihn[†]

[†]Solid State Physics Laboratory, ETH Zürich, CH-8093 Zürich, Switzerland

[‡]Institut für Theoretische Physik, Universität Regensburg, D-93040 Regensburg, Germany

[§]Department of Physics, National Cheng Kung University, Tainan 70101, Taiwan

[∥]Advanced Materials Laboratory, National Institute for Material Science, 1-1 Namiki, Tsukuba 305-0044, Japan

[⊥]National Graphene Institute, University of Manchester, Manchester M13 9PL, United Kingdom

Supporting Information

ABSTRACT: We report on the observation of magnetoresistance oscillations in graphene p−n junctions. The oscillations have been observed for six samples, consisting of single-layer and bilayer graphene, and persist up to temperatures of 30 K, where standard Shubnikov−de Haas oscillations are no longer discernible. The oscillatory magnetoresistance can be reproduced by tight-binding simulations. We attribute this phenomenon to the modulated densities of states in the n- and p-regions.

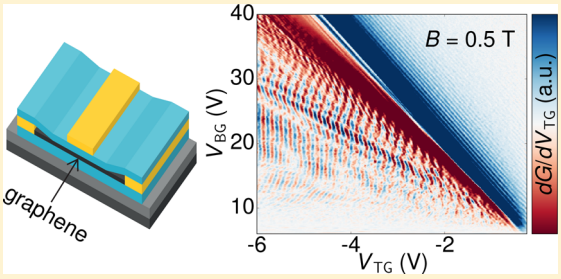

KEYWORDS: *Graphene, ballistic transport, p−n junction, magnetoresistance*

A p−n junction is one of the basic building blocks of any electronic circuit. The ambipolar nature of graphene provides a flexible way to induce p−n junctions by electrostatic gating. This offers an opportunity to tune the charge carrier densities in the n- and p-doped regions independently. The potential gradient across a p−n interface depends on the thickness of the involved insulators and can also be modified by appropriate gate voltages. Due to the high electronic quality of present day graphene devices, a number of transport phenomena in pnp or npn junctions have been reported, such as ballistic Fabry-Pérot oscillations[1−3] and so-called snake states,[4,5] both of which depend on characteristic length scales of the sample.

Here we report the discovery of yet another kind of oscillation, which does not depend on any such length scale. The oscillations occur in the bipolar regime, in the magnetic field range where Shubnikov−de Haas oscillations are observed in the unipolar regime. These novel oscillations in the bipolar regime are governed by the unique condition that the distance between two resistance minima (or maxima) in gate voltage space is given by a constant filling factor difference of $\Delta\nu = 8$. The features are remarkably robust: they occur in samples with one and two p−n interfaces; in single and bilayer graphene; up to temperatures of 30 K (where Shubnikov−de Haas oscillations have long disappeared); over a large density range; for interface lengths ranging from 1 to 3 μm, and in both pnp and npn regimes. The oscillations have been observed in a magnetic field range of $B = 0.4$ T up to $B = 1.4$ T. Their periodicity does not match the periodicity of the aforementioned snake states. In this paper we address this phenomenon and suggest a model which can qualitatively explain the oscillations.

Measurements were performed on six samples in total, which all consist of a graphene flake encapsulated between two hexagonal boron nitride (h-BN) flakes on a Si/SiO_2 substrate. They all show similar behavior. This paper focuses on measurements performed on one sample (sample A), with the device geometry sketched in Figure 1a. Specifications of the other five samples are summarized in Table 1. The bilayer graphene (BLG) flake was encapsulated with the dry transfer technique described in ref 6. A top gate was evaporated on the middle part of the sample, which divides the device into two outer regions, only gated by the back gate (single-gated regions), and the dual-gated middle region. The other five samples were made with the more recent van der Waals pick-up technique.[7] Unless stated otherwise, the measurements were performed at 1.7 K. An AC voltage bias of 50 μV was applied symmetrically between the Ohmic contacts ("source" and "drain" in Figure 1a, inner contacts in Figure 1b) and the current between the same contacts was measured. The

Received: December 22, 2016
Revised: February 27, 2017
Published: April 6, 2017

DOI: 10.1021/acs.nanolett.6b05318
Nano Lett. 2017, 17, 2852−2857

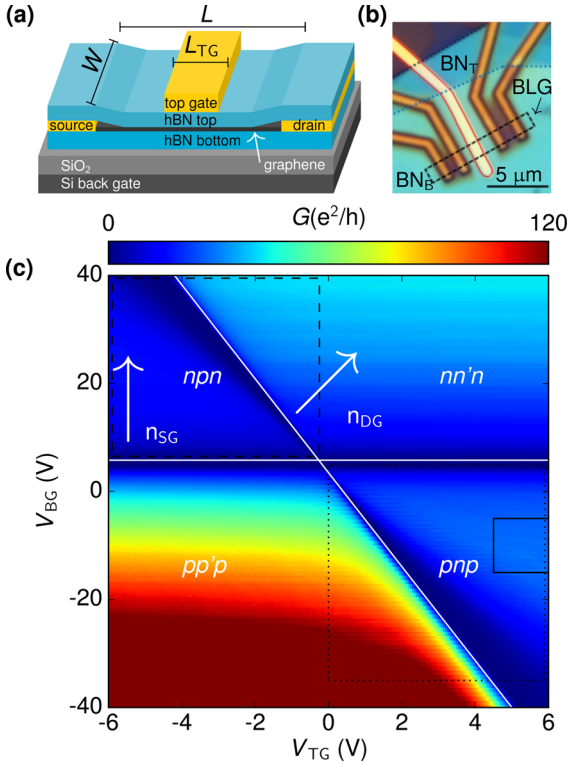

Figure 1. Characterization of the device. (a) Schematic of the device: a bilayer graphene flake is encapsulated between h-BN layers. It is contacted by Au contacts, and a Au top gate is patterned on top, which defines the dual-gated region. (b) Optical microscope image of the sample. The four contacts, of which only the inner ones were used, appear orange. The top gate is outlined by a red curve. (c) Conductance of the sample at B = 0 T, T = 1.7 K. Four regions of different polarities are indicated. A zoom of the transconductance in the boxed region with a solid line is shown in Figure 2. The dashed (dotted) box indicates the gate voltage range in which Figure 3a,b (d,e) were measured.

Table 1. Characteristics of Samples A–F

sample name	A	B	C	D	E	F
sample width W (μm)	1.3	1.4	1.1	0.9	3	1.2
sample length L (μm)	3.0	1.4	1.0	2.3	3	2.8
top gate length L_{TG} (μm)	1.1	0.7	0.55	1.2	1.0	1.0
distance to top gate (nm)	23	44	28	57	35	25
number of graphene layers	2	1	2	2	2	2
junction type	npn	pn	npn	pn	npn	npn

transconductance dG/dV_{TG} was measured by applying an AC modulation voltage of 20 mV to the top gate.

Figure 1c shows the conductance as a function of top gate voltage V_{TG} and back gate voltage V_{BG}. Charge neutrality of the single-gated regions shows up as a horizontal line of low conductance and is marked by a white line. The diagonal line of low conductance corresponds to charge neutrality of the dual-gated region. The slope of this line is given by the capacitance ratio of the top and back gate. Together these lines divide the map into four regions with different combinations of carrier types: two with the same polarities in the single- and dual-gated regions (pp'p and nn'n) and two with different polarities (npn and pnp). The conductance in the latter regions shows a modulation which is more clearly visible in the transconductance (see Figure 2a). The oscillatory conductance is

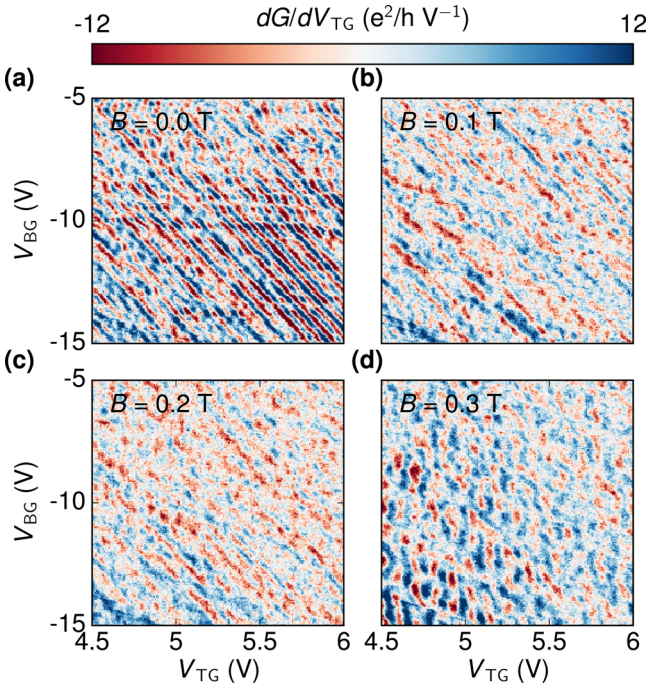

Figure 2. Disappearance of Fabry–Pérot oscillations with increasing magnetic field. The measurement was taken in the boxed region with solid lines in Figure 1c. At B = 0 T (a) the transconductance shows clear Fabry–Pérot oscillations. They disappear in a magnetic field of $B \gtrsim 0.1$ T (b–d).

caused by Fabry-Pérot interference of charge carriers traveling back and forth in the region of the sample underneath the top gate. Their periodicity yields a cavity length L_{TG} = 1.1 μm, which is in agreement with the lithographic length of the top gate. The Fabry–Pérot oscillations were studied in more detail in ref 3, which revealed the ballistic nature of transport in the dual-gated region.

The Fabry–Pérot oscillations disappear in a magnetic field of $B \gtrsim 100$ mT (see Figure 2b–d). Yet at magnetic fields of B = 0.4 T, a new oscillatory pattern appears in the npn and pnp regime. This can be seen in the conductance and transconductance maps recorded at B = 0.5 T, shown in Figure 3a,b,d,e. The oscillations follow neither the horizontal slope of features taking place in the single-gated region nor the diagonal slope of the dual-gated region. They are therefore expected to occur at the interface between the p- and n-doped regions. This was confirmed by measurements on sample D, which had two contacts in the single-gated region and two contacts in the dual-gated region. For this sample, only the conductance along paths involving the interface shows oscillations (see Supporting Information).

On top of this novel oscillatory pattern the transconductance of sample A in Figure 3b(e) shows faint diagonal lines in the nn'n(pp'p) regime, which are Shubnikov–de Haas oscillations in the dual-gated region. The occurrence of Shubnikov–de Haas oscillations shows that in this moderate magnetic field regime the Landau levels are broadened by disorder on the scale of their spacing, resulting in a modulation of the density of states.

Using a plate capacitor model described in the Supporting Information of ref 3, the gate voltage axes can be converted into density and filling factor axes, ν_X with X = SG, DG for the single- and dual-gated regions, respectively. The result of this

DOI: 10.1021/acs.nanolett.6b05318
Nano Lett. 2017, 17, 2852–2857

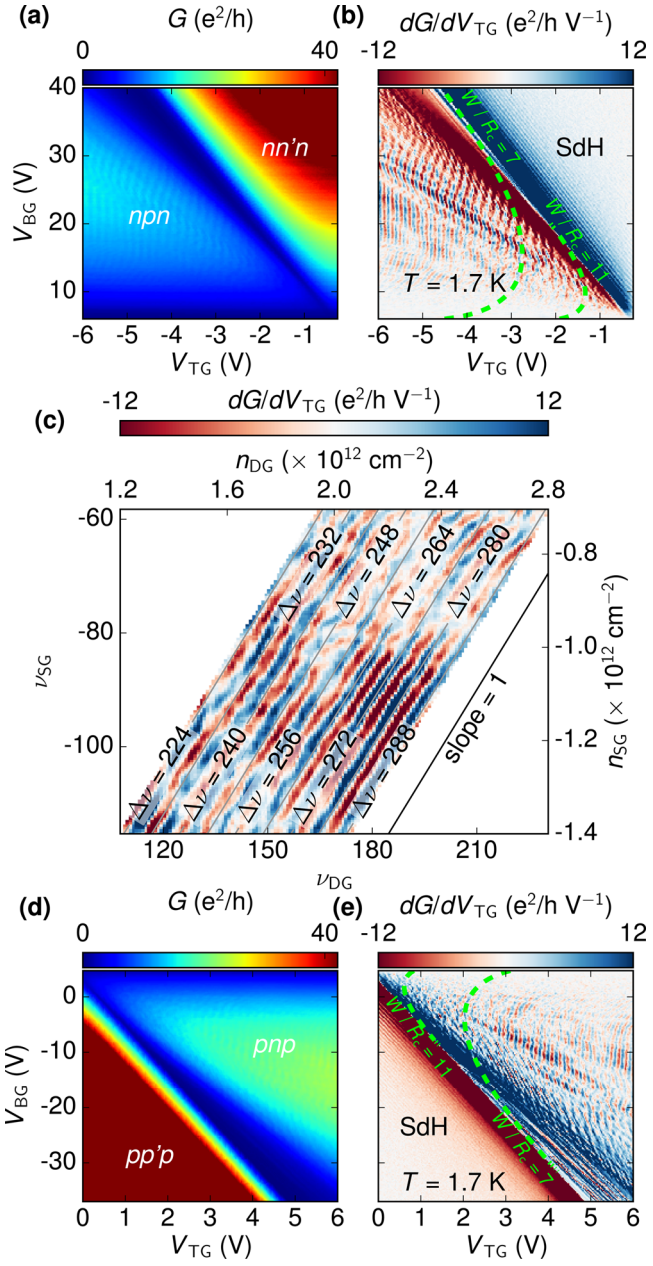

Figure 3. Magnetotransport at B = 0.5 T. (a) Conductance of the sample at 0.5 T, showing an oscillatory pattern in the npn regime. The measurement was taken in the dashed boxed region of Figure 1c. (b) The oscillatory pattern in the npn regime is more clearly visible in the transconductance. Green dashed lines indicate the pattern expected for snake states. In the nn'n regime some faint lines can be distinguished, following the slope of the charge neutrality line of the dual gated region. These are Shubnikov–de Haas oscillations. (c) Transconductance at B = 0.5 T in the pnp regime as a function of charge carrier density (and filling factor) in the single- and dual-gated region. The oscillatory pattern follows the indicated line of slope one and can therefore be described by lines of constant filling factor difference $\Delta\nu = \nu_{DG} - \nu_{SG}$. (d, e) Same as a, b, but with opposite charge carrier polarities. The oscillations are essentially particle–hole symmetric.

transformation is shown in Figure 3c. The oscillatory pattern has a slope of 1; i.e., it follows lines of constant filling factor difference $\Delta\nu = \nu_{SG} - \nu_{DG}$. It appears that the oscillations can be described by

$$G = \langle G \rangle + A \cos\left(2\pi \frac{\Delta\nu}{8}\right) \quad (1)$$

where A is the amplitude of the oscillations, which is on the order of 4% of the background conductance $\langle G \rangle$ at T = 1.7 K. The distance between one conductance maximum and the next can therefore be bridged by either changing the filling factor in one region by 8, or by changing the filling factor in both regions oppositely by 4. It should be noted that eq 1 can be used to describe the oscillations in all six samples, regardless of the number of graphene layers and the sample width (see Table 1 and the Supporting Information).

The oscillations persist in magnetic fields up to B = 1 T for sample A and the periodicity scales with $\Delta\nu$ for the entire magnetic field range. In higher magnetic fields the conductance is dominated by quantum Hall edge channels and takes on values below e^2/h in the npn and pnp regimes, in agreement with observations by Amet et al.[8] Other works report on the (partial) equilibration of edge channels[8−13] and shot noise[14,15] in p−n junctions in the quantum Hall regime.

The oscillatory conductance is quite robust against temperature changes. Figure 4a,b shows the decay of the amplitude as a function of temperature T. The oscillatory conductances in the pnp and npn regime disappear at a temperature around T = 30 K. As can be seen in Figure 4c, at T = 10 K the oscillations are still clearly present, while the Shubnikov–de Haas oscillations in the pp'p regime have already faded out. The

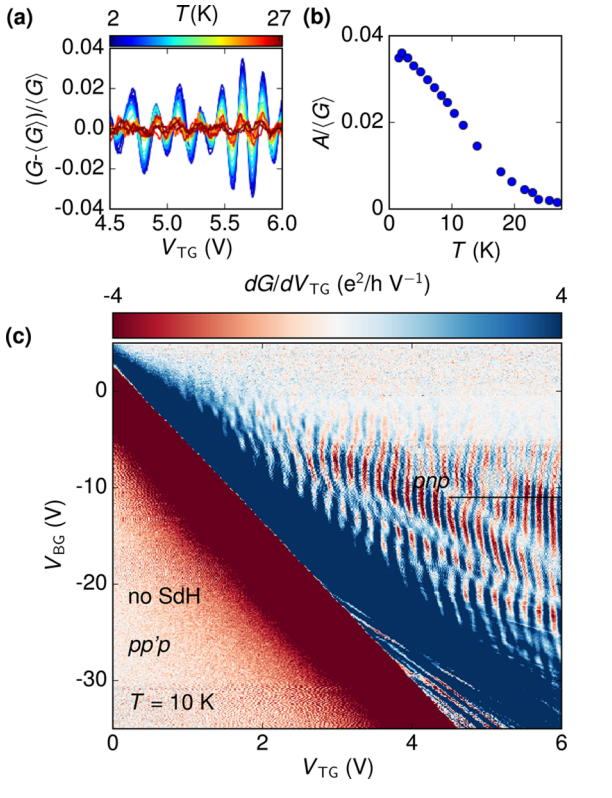

Figure 4. Temperature dependence. (a) Oscillatory part of the conductance as a function of top gate voltage and temperature measured along the line cut indicated by the black line in panel c. (b) Amplitude A of the oscillatory conductance as a function of temperature. The oscillations disappear around T = 30 K. (c) Transconductance at T = 10 K, B = 0.5 T in the pnp regime. Whereas Shubnikov–de Haas oscillations in the pp'p regime have faded out, the oscillatory pattern in the pnp regime persists.

DOI: 10.1021/acs.nanolett.6b05318
Nano Lett. 2017, 17, 2852−2857

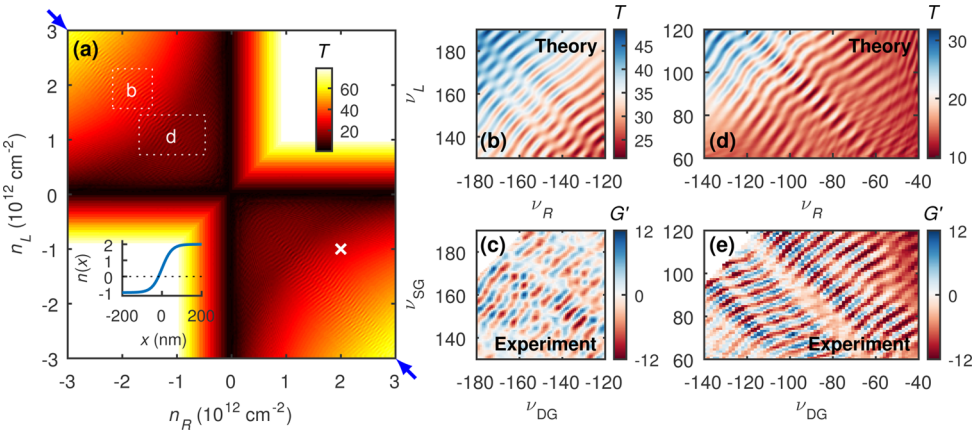

Figure 5. (a) Transmission T as a function of the carrier densities on the left, n_L, and right, n_R, for an ideal SLG p−n junction at a perpendicular magnetic field B = 0.5 T based on a tight-binding transport calculation (color range restricted for clarity). Oscillations occur in the vicinity of the symmetric bipolar axis marked by blue arrows. Inset: an example of the considered carrier density profile corresponding to the white cross. White dashed boxes correspond to the density regions shown in panels b and d, where the carrier density values are transformed in filling factors. (c/e) Transconductance G' measured for sample B/E shown with the same filling factor range as panels b/d.

persistence up to T = 30 K indicates that the studied phenomenon does not require phase coherence on the scale of the device size. The phase coherence length at T = 1.7 K is estimated to be on the order of the device size, but it falls off with $1/T$.[16]

The above-discussed oscillations can be reproduced by transport calculations for an ideal SLG p−n junction at an intermediate magnetic field B, based on the scalable tight-binding model.[17] The ideal junction is modeled by connecting two semi-infinite graphene ribbons (oriented along armchair) with their carrier densities given by n_L in the far left and n_R in the far right. A simple hyperbolic tangent function with smoothness 50 nm bridging n_L and n_R is considered; see the inset of Figure 5a for an example. To cover the density range up to $\pm 3 \times 10^{12}$ cm^{-2} corresponding to a maximal Fermi energy of $E_{max} \approx 0.2$ eV, the scaling factor s_f = 10 is chosen because it fulfills the scaling criterion[17] $s_f \ll 3\, t_0\, \pi/E_{max} \approx 141$ very well; here $t_0 \approx 3$ eV is the hopping energy of the unscaled graphene lattice. Note that the following simulations consider W = 1 μm for the width of the graphene ribbon, but simulations based on a different width show an identical oscillation behavior (see Supporting Information for details), confirming its width-independent nature as already concluded from our measurements.

The transmission function $T(n_R, n_L)$ across the ideal p−n junction at B = 0.5 T is shown in Figure 5a, where fine oscillations along symmetric bipolar axis (marked by the blue arrows) from np to pn through the global charge neutrality point can be seen. Two regions marked by the white dashed boxes in Figure 5a are zoomed-in and shown in Figure 5b and d for a closer look and comparison with the measurements of sample B and E (Figure 5c and e, respectively). Despite certain phase shifts (observed in Figure 5b, d, and e) that are beyond the scope of the present study, good agreement between our transport simulation and experiment showing the oscillation period well fulfilling eq 1 can be seen.

Other works[4,5] report on the formation of so-called snake states along p−n interfaces in graphene. Snake states result in a minimum in the conductance whenever the sample width W and the cyclotron radius R_c satisfy $W/R_c = 4m - 1$ with m a positive integer. In the density range of Figure 3b,e this would lead to two resonances at most (indicated by green dashed lines in Figure 3b,e), which is far less than the observed number of resonances. On top of that, snake states are inconsistent with the observed absence of a dependence on sample width. Furthermore, the tight-binding simulation also confirms that the observed effect is independent of the sample width and cannot be suppressed by introducing strong lattice defects in the vicinity of the p−n junction (see Supporting Information). We therefore rule out snaking trajectories as a possible cause of the observed oscillations.

Another process which could give rise to oscillations in a graphene p−n junction in a magnetic field is the interference of charge carriers which are partly reflected and partly transmitted at the interface. When the charge carrier densities are equal on both sides of the interface, electrons and holes will have equal cyclotron radii, and therefore the paths of transmitted and reflected charge carriers will form closed loops. For the case of equal density, this model predicts the right periodicity of the oscillations.[18] Experimentally, however, the measured oscillations are still visible when the densities on both sides of the p−n interface are quite different: at the point (V_{BG},V_{TG}) = (12,−6) V for example (see Figure 3b), the cyclotron radii on the p and n side are respectively 0.36 and 0.16 μm. The path lengths hence differ by $2\Delta R_c$ = 0.40 μm, which is more than seven times the Fermi wavelength (0.02 and 0.05 μm). It seems unlikely that interference between charge carriers on skipping orbits can still occur in this density regime. On top of that, the tight-binding simulations show that the oscillatory pattern is still present when introducing large-area lattice defects in the vicinity of the p−n junction, which destroy the skipping trajectories (see Supporting Information). The observed robustness against temperature changes is in contradiction with this model as well. Thus, the observed oscillations cannot be ascribed to the interference of charge carriers on cyclotron orbits at the p−n interface.

Since the oscillations occur in both single-layer and bilayer graphene, we exclude an explanation that relies on specific details of the dispersion relation. In the magnetic field range where the oscillations are observed, the sample width is comparable to the classical cyclotron diameter. This excludes explanations based on classical electron flow following skipping orbit-like motion along edges.

DOI: 10.1021/acs.nanolett.6b05318
Nano Lett. 2017, 17, 2852−2857

A mechanism which may cause the oscillations involves the alignment of the density of states (DOS) around the Fermi energy. Diagrams of the DOS in the single- and dual-gated regions are sketched in Figure 6a–c. Figure 6d shows a zoom in

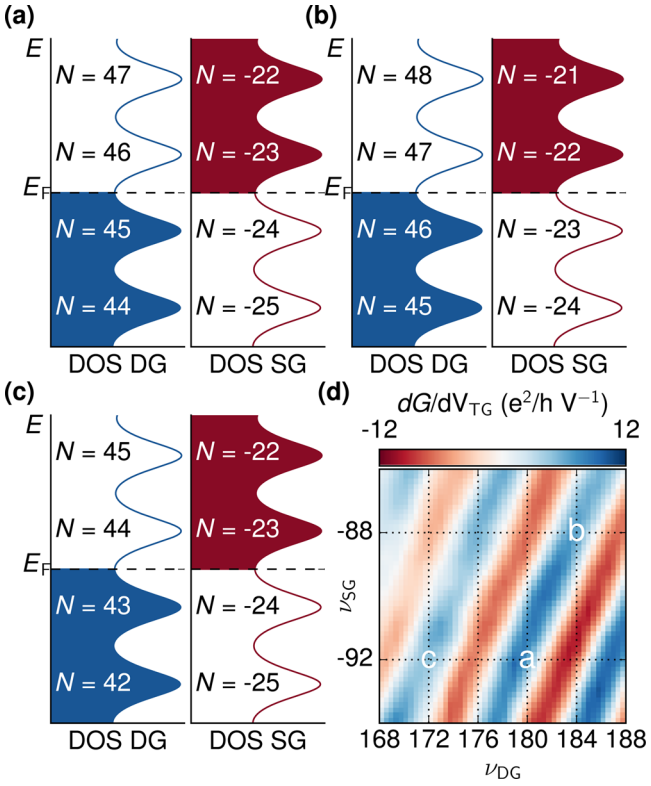

Figure 6. (a–c) Schematics of the densities of states as a function of energy for the single- and dual-gated regions of the sample at positions a–c of the measurement. (d) Zoom in Figure 3c. The alignment of the densities of states can lead to an oscillatory pattern with the right slope: along the line from point a to point b the two combs of densities of states stay aligned, whereas the combs shift with respect to one another when moving from point a to point c.

the map of the oscillatory transconductance of Figure 3c. At point a in this zoom the filling factor in the dual-gated regime is $\nu_{DG} = 180$ and $\nu_{SG} = -92$ in the single-gated region. Because of the 4-fold degeneracy of the Landau levels, Landau level numbers are $N = 45$ and $N = -23$, respectively, as shown in the DOS diagram of Figure 6a. When following the oscillatory pattern from point a to point b, the two combs of DOS remain aligned with one another, and only the Fermi level changes. This in contrast to what happens when moving from point a to point c: the DOSs shift with respect to one another, and the transconductance oscillates. It could therefore be the case that the alignment of the DOS affects the conductance of the p–n interface in a way similar to the magneto-intersubband oscillations (MISO) of a two-dimensional electron gas (2DEG):[19,20] the occupation of two of the energy subbands of a 2DEG can lead to enhanced scattering between the subbands when the DOSs of the subbands are aligned. Although the p- and n-regions are spatially separated in the case of graphene p–n junctions, a similar enhancement of the coupling at the interface may be observed. In the pp'p and nn'n regime the interfaces are much more transparent (see conductance in Figure 4a,d and ref 21); therefore, the interface plays a negligible role in the total conductance. This explains why the oscillations are only visible in the presence of a p–n interface. As the two outer regions of the sample have the same density up to an insignificant difference in residual doping, the two interfaces contribute in a similar way. The number of interfaces can at most influence the visibility of the oscillations. In practice we find that the visibility is however mostly influenced by sample quality. Just as for the oscillations we report on, MISO persist up to relatively high temperatures. The spacing predicted by this model lacks a factor of 2 compared to the experiment, however: it would predict the argument of the cosine of eq 1 to be $2\pi\Delta\nu/4$. Further investigations are needed to explain this discrepancy between the MISO model on the one hand and the experimental data and the tight-binding simulations on the other hand.

In conclusion, we have observed oscillations in the conductance of six graphene p–n junctions in the magnetic field range of $B = 0.4$–1.5 T. The oscillations are independent of sample width and can be described by the filling factor difference between the single- and the dual-gated regions. The oscillations are quite robust against temperature changes: they fade out only in the range of $T = 20$–40 K, whereas Shubnikov–de Haas oscillations decay below $T = 10$ K. The oscillations can be well-reproduced by tight-binding transport calculations considering an ideal p–n junction at a constant magnetic field. Up to a factor of 2, the oscillatory pattern can be explained by considering the density of states alignment of the single- and dual-gated regions.

■ ASSOCIATED CONTENT

Supporting Information

The Supporting Information is available free of charge on the ACS Publications website at DOI: 10.1021/acs.nanolett.6b05318.

Tight binding simulations and magnetoresistance oscillations in samples B–F (PDF)

■ AUTHOR INFORMATION

Corresponding Author

*E-mail: overwegh@phys.ethz.ch.

ORCID

Hiske Overweg: 0000-0002-9107-4763

Notes

The authors declare no competing financial interest.

■ ACKNOWLEDGMENTS

We thank Péter Makk and François Peeters for fruitful discussions. We acknowledge financial support from the European Graphene Flagship and the Swiss National Science Foundation via NCCR Quantum Science and Technology. M.-H.L. and K.R. acknowledge financial support by the Deutsche Forschungsgemeinschaft within SFB 689.

■ ABBREVIATIONS

h-BN, hexagonal boron nitride; BLG, bilayer graphene; TG, top gate; BG, back gate; SG, single-gated; DG, dual-gated; SLG, single layer graphene; DOS, density of states; MISO, magneto-intersubband oscillations; 2DEG, two-dimensional electron gas

■ REFERENCES

(1) Grushina, A. L.; Ki, D.-K.; Morpurgo, A. F. *Appl. Phys. Lett.* **2013**, *102*, 223102.

DOI: 10.1021/acs.nanolett.6b05318
Nano Lett. 2017, 17, 2852–2857

(2) Rickhaus, P.; Maurand, R.; Liu, M.-H.; Weiss, M.; Richter, K.; Schönenberger, C. *Nat. Commun.* **2013**, *4*, 2342.
(3) Varlet, A.; Liu, M.-H.; Krueckl, V.; Bischoff, D.; Simonet, P.; Watanabe, K.; Taniguchi, T.; Richter, K.; Ensslin, K.; Ihn, T. *Phys. Rev. Lett.* **2014**, *113*, 116601.
(4) Taychatanapat, T.; Tan, J. Y.; Yeo, Y.; Watanabe, K.; Taniguchi, T.; Özyilmaz, B. *Nat. Commun.* **2015**, *6*, 6093.
(5) Rickhaus, P.; Makk, P.; Liu, M.-H.; Tóvári, E.; Weiss, M.; Maurand, R.; Richter, K.; Schönenberger, C. *Nat. Commun.* **2015**, *6*, 6470.
(6) Dean, C. R.; Young, A. F.; Meric, I.; Lee, C.; Wang, L.; Sorgenfrei, S.; Watanabe, K.; Taniguchi, T.; Kim, P.; Shepard, K. L.; et al. *Nat. Nanotechnol.* **2010**, *5*, 722−6.
(7) Wang, L.; Meric, I.; Huang, P. Y.; Gao, Q.; Gao, Y.; Tran, H.; Taniguchi, T.; Watanabe, K.; Campos, L. M.; Muller, D. A.; et al. *Science* **2013**, *342*, 614−7.
(8) Amet, F.; Williams, J. R.; Watanabe, K.; Taniguchi, T.; Goldhaber-Gordon, D. *Phys. Rev. Lett.* **2014**, *112*, 1−5.
(9) Williams, J. R.; Dicarlo, L.; Marcus, C. M. *Science* **2007**, *317*, 638.
(10) Özyilmaz, B.; Jarillo-Herrero, P.; Efetov, D.; Abanin, D. A.; Levitov, L. S.; Kim, P. *Phys. Rev. Lett.* **2007**, *99*, 2−5.
(11) Ki, D. K.; Nam, S. G.; Lee, H. J.; Özyilmaz, B. *Phys. Rev. B: Condens. Matter Mater. Phys.* **2010**, *81*, 1−4.
(12) Morikawa, S.; Masubuchi, S.; Moriya, R.; Watanabe, K.; Taniguchi, T.; Machida, T. *Appl. Phys. Lett.* **2015**, *106*, 183101.
(13) Tóvári, E.; Makk, P.; Rickhaus, P.; Schönenberger, C.; Csonka, S. *Nanoscale* **2016**, *8*, 11480−11486.
(14) Kumada, N.; Parmentier, F. D.; Hibino, H.; Glattli, D. C.; Roulleau, P. *Nat. Commun.* **2015**, *6*, 8068.
(15) Matsuo, S.; Takeshita, S.; Tanaka, T.; Nakaharai, S.; Tsukagoshi, K.; Moriyama, T.; Ono, T.; Kobayashi, K. *Nat. Commun.* **2015**, *6*, 8066.
(16) Engels, S.; Terrés, B.; Epping, A.; Khodkov, T.; Watanabe, K.; Taniguchi, T.; Beschoten, B.; Stampfer, C. *Phys. Rev. Lett.* **2014**, *113*, 1−5.
(17) Liu, M.-H.; Rickhaus, P.; Makk, P.; Tóvári, E.; Maurand, R.; Tkatschenko, F.; Weiss, M.; Schönenberger, C.; Richter, K. *Phys. Rev. Lett.* **2015**, *114*, 1−5.
(18) Patel, A. A.; Davies, N.; Cheianov, V.; Fal'ko, V. I. *Phys. Rev. B: Condens. Matter Mater. Phys.* **2012**, *86*, 1−4.
(19) Raikh, M.; Shahbazyan, T. *Phys. Rev. B: Condens. Matter Mater. Phys.* **1994**, *49*, 5531−5540.
(20) Dmitriev, I. A.; Mirlin, A. D.; Polyakov, D. G.; Zudov, M. A. *Rev. Mod. Phys.* **2012**, *84*, 1709−1763.
(21) Rickhaus, P.; Liu, M.-H.; Makk, P.; Maurand, R.; Hess, S.; Zihlmann, S.; Weiss, M.; Richter, K.; Schönenberger, C. *Nano Lett.* **2015**, *15*, 5819−5825.

DOI: 10.1021/acs.nanolett.6b05318
Nano Lett. 2017, 17, 2852−2857